PHYSICAL REVIEW A VOLUME 36, NUMBER 12 DECEMBER 15, 1987

Collective effects in laser multiphoton ionization

F. Giammanco
Dipartimento di Fisica, Universita di Pisa, Piazza Torricelli, 2 56100 Pisa, Italy
(Received 16 March 1987)

The time-space behavior of the charges produced in typical laser multiphoton ionization experiments is analyzed from the point of view of the fluid approximation. On the basis of analytic methods, first the equation system describing the one-dimensional motion of a single-charged fluid in an external uniform and constant electric field is solved. It is shown that the solution can be extended to the three-dimensional case, also including momentum-exchange collisions and time-varying electric field and temperature. Moreover, the method is extended to analyze the motion of both ions and electrons, coupled by the self-generated electric field. Finally, the consequences on the time-space behavior of the collected current, in typical multiphoton ionization experiments, are pointed out and the range of validity also discussed.

I. INTRODUCTION

Laser multiphoton ionization (MPI) is a spectroscopic technique widely used in several fields of investigation as, for instance, trace analysis, isotope separation by selective ionization, laser-induced chemical reactions, and so on. MPI has been largely investigated and new phenomena, such as above-threshold ionization (ATI), have been recently discovered.[1]

In spite of the different purposes, many features are common to all MPI experiments. In fact, the ionized yields are collected by externally applied electric and/or magnetic fields and the induced current is either totally detected by the so-called optogalvanic technique or mass (or energy) analyzed by appropriate spectrometers.

MPI involves, usually, pulsed lasers and, except for particular experiments involving very high electric fields,[2] the response time of the collection scheme is much longer than the laser interaction time (0.1–10 ns). Hence, during the collection time, many effects, to be classified schematically as atomic interactions and collective phenomena, can modify the initial parameters (number density, temperature, velocity distribution) of the laser-produced yields. Whereas the atomic interactions, typically binary collisions, are effective only over a short distance, the collective phenomena may act on a macroscopic scale and therefore may drastically change the shape of the collective current, the time of flight through the spectrometer, and so on. The phenomenon of "electron trapping," recently introduced to explain an anomalous behavior of the ATI electronic spectrum as the initial density of the ionized yields increases,[3–8] may be also considered as an example of a collective interaction, depending on the self-generated fields.

The fluid approximation[9] is an appropriate approach for a wide class of experiments. The equations that constitute this approximation are derived from the Boltzmann transport equation, such as the momenta of different order, averaged on an isotropic velocity distribution,[9] and so they describe the time-space evolution of the fluid mean quantities (velocity, density, and energy) referred to the laboratory frame.

In general, the electron-electron collision time is shorter than the collection time and thus the initial distribution quickly approaches a Maxwell distribution. Nevertheless, the usual fluid approximation can be also extended to the class of the collisionless MPI plasmas. In fact, it will be demonstrated that the derivation of the fluid equations requires only having zero for the particle velocity averaged over the distribution function.

In ATI experiments, several authors[10–14] have measured the angular distribution as a function of the angle between the directions of the laser polarization and the detection. The observed distribution is strongly peaked along the laser polarization and the sharpness increases as the order of the peaks increases. In any case, along any axis there are two equiprobable opposite directions for the ejected electrons and that assures a mean zero velocity. Hence, in the collisionless case, the electron kinetic energy term kT_e of the fluid equations will be given by the initial electron energy E_e equal to the difference between the absorbed laser photons ($nh\nu$) and the ionization potential (i): $E_e = nh\nu - i$ (see Sec. II).

It turns out that the general solution of the fluid equation system, which also includes the self-consistent fields and the atomic processes, is a formidable problem. Thus, solutions are obtained when some assumptions, depending on the characteristics of the problem, are introduced in the equation system, of course with loss of generality. Particularly in the laser plasmas produced by the MPI process, the usual plasma physics approximations of linearization, uniform density, and so on do not correspond to the physical reality. In fact, owing to the strong field and density gradients and the fast time evolution, all the nonlinear terms and all the time-space derivatives must be retained in the exact description.

In spite of the general features involved in the theoretical analysis and the good reproducibility of the experimental samples, the atomic physics approach to MPI-produced plasma has been considered, in general, as a trouble to avoid, if possible. On the contrary, the plasma physics point of view should be used to determine

the main features. Actually, with regard to the electron densities and energies involved, these plasmas are similar to those produced by means of the old plasma sources, whose research was progressively abandoned as a consequence of the increasing interest in the nuclear fusion field. In fact, the MPI plasmas can also be classified as tenuous, non-neutral, unstable, and, in many cases, collisional (with neutral particles) plasmas. Compared with the "old plasmas," the MPI ones exhibit good reproducibility, high repetition rate, and a more reliable control of the initial parameters. Hence, it seems that MPI plasmas could be considered, from the plasma physics point of view, as suitable samples to study nonlinear interactions. This work presents a solution of the fluid equations, on the basis of analytic methods, under some hypotheses that in general correspond well with the physical reality of the MPI experiments. The plan of the paper is the following. Firstly, the method is applied to solve the equations describing the unidimensional motion of a single-charged fluid in an external uniform electric field. It is supposed that the laser MPI produces an initial Gaussian-shaped density profile of ionized yields. All the processes changing the number density in the continuity equation will be neglected.

In Sec. III it will be shown that the solution of the unidimensional case can be easily extended to a tridimensional case and that momentum-exchange collisions, time-varying electric field, and time-varying temperature may be included in the solution. As a further consequence, the previous analytical solution will be applied to solve the magnetohydrodynamic (MHD) equations for the plasma motion in an electric field (Sec. IV). In Sec. V, by an approximate approach, including the self-generated internal field, the method will be extended to solve the coupled two-fluid equations. Finally, following the previous descriptions, the consequences of the time-space behavior of the macroscopic collected current, in typical MPI experiments, will be pointed out and the range of validity also discussed (Sec. VI).

II. METHOD OF SOLUTION

As recalled in the Introduction, the fluid equations are obtained from the Boltzmann transport equation as momenta of different order. That Boltzmann equation describes the time evolution of the particle distribution function $f(\mathbf{r},\mathbf{w},t)$ in phase space. In the absence of collisions among particles of different kind, the total derivative of f is zero[9] and thus the Boltzmann equation is represented by

$$\frac{df}{dt}=\frac{\delta f}{\delta t}+\sum_j w_j\frac{\delta f}{\delta x_j}+\frac{1}{m}\sum_j F_j\frac{\delta f}{\delta w_j}=0\ , \tag{1}$$

where x_j and w_j are the j components of the particle position and velocity and F_j the j component of the force acting on the particle. Assuming that the particle density is $n(\mathbf{r},t)=\int f\,d^3w$, where $d^3w=dw_x dw_y dw_z$, the mean value of a quantity $Q(\mathbf{w})$ (either scalar or vectorial) is given by

$$Q(\mathbf{r},t)=\langle Q(\mathbf{w})\rangle=[1/n(\mathbf{r},t)]\int Q(\mathbf{w})f\,d^3w\ . \tag{2}$$

By multiplying by $Q(\mathbf{w})$ and integrating on the velocity space, Eq. (1) is transformed into an equation describing the time evolution of $Q(\mathbf{w})$, that is,

$$\frac{\delta}{\delta t}[n\langle Q(\mathbf{w})\rangle]+\sum_j\frac{\delta}{\delta x_j}[n\langle Q(\mathbf{w})w_j\rangle]$$

$$-(1/m)\sum_j\left\langle\frac{\delta}{\delta w_j}F_jQ(\mathbf{w})\right\rangle=0\ . \tag{3}$$

In the derivation of Eq. (3), the only requirement is to have a symmetric distribution function.

The zeroth-order momentum corresponds to $Q(\mathbf{w})=1$. From Eq. (3), the resulting equation describes the macroscopic evolution of the density, the third term in Eq. (3) being zero because the j component of the force is independent of the j component of the velocity,

$$\frac{\delta}{\delta t}n+\nabla\cdot(n\mathbf{v})=0\ , \tag{4}$$

where

$$\mathbf{v}(\mathbf{r},t)=\langle\mathbf{w}\rangle=[1/n(\mathbf{r},t)]\int\mathbf{w}f\,d^3w$$

is the mean fluid velocity.

The position $Q(\mathbf{w})=m\mathbf{w}$ leads to the momentum-transfer (motion) equation. It is worthwhile to express the velocity $\mathbf{w}$ as a sum of the fluid velocity $\mathbf{v}$ and the "random" velocity $\mathbf{u}$. As recalled in the Introduction, $\langle\mathbf{u}\rangle=0$ also for monochromatic electrons produced in ATI experiments.

The first and the third terms of Eq. (3) immediately lead, respectively, to $m(\delta/\delta t)(n\mathbf{v})$ and $n\mathbf{F}$. The second term requires a more detailed discussion. By using the previous position for $\mathbf{w}$, the second term is transformed into

$$nm\mathbf{v}(\nabla\cdot\mathbf{v})+m(\mathbf{v}\cdot\nabla)(n\mathbf{v})+m\nabla\overleftrightarrow{\Phi}=m\nabla(n\langle\mathbf{ww}\rangle)\ , \tag{5}$$

where the condition $\langle\mathbf{u}\rangle=0$ has been used to eliminate the terms $\langle\mathbf{vu}\rangle$ and $\langle\mathbf{uv}\rangle$. The symbol $\leftrightarrow$ represents a tensor and, particularly, $\overleftrightarrow{\Phi}$ is the stress tensor, whose components are defined by $\Phi_{ij}=mn\langle u_iu_j\rangle$. For a Maxwell distribution, the off-diagonal elements are zero and the diagonal terms are equal to the fluid pressure, i.e., $\nabla\overleftrightarrow{\Phi}=\nabla P=\nabla(nkT)$. For ATI-produced electrons, if one-dimensional motion is assumed (along the direction of the laser polarization), all terms are zero except a quadratic term along the laser polarization, i.e., $nmu^2=2nE_e$, where E_e corresponds to the electron kinetic energy. In a three-dimensional expansion, the diagonal terms are still equal to $2nE_e$ and the angular distribution of electrons must be included in n.

By using Eq. (5) and the continuity equation (4), the motion equation becomes

$$\frac{\delta}{\delta t}\mathbf{v}+(\mathbf{v}\cdot\nabla)\mathbf{v}=\frac{\mathbf{F}}{m}-\frac{\nabla P}{mn}\ , \tag{6}$$

where the symbols are previously defined.

From the previous discussion, the motion and continuity equations describing the one-dimensional motion

of a single-charged species (either ions or electrons) in an external electric field are, respectively,

$$\frac{\delta v}{\delta t}+v\frac{\delta v}{\delta x}=A_0-(kT/m)\frac{\delta}{\delta x}\ln(n)\ , \tag{7}$$

$$\frac{\delta n}{\delta t}+\frac{\delta}{\delta x}(nv)=0\ , \tag{8}$$

where $A_0=(q/m)E_0$. T,q,m are, respectively, the temperature, charge (including the sign), and mass of the selected species and E_0 is the electric field.

The initial conditions are $v(x,0)=0$ and $n=n_0\exp[-(x/\delta)^2]$. A further additional assumption is $\delta T/\delta x=0$. Such a hypothesis is very well satisfied in the MPI experiments, where the initial electron kinetic energy depends on the difference between the energies of the absorbed photons and the ionization potential.

Dividing Eq. (8) by n, it turns out that the system depends on v and $\ln(n)$. Both the functions v and $\ln(n)$ admit Taylor developments in a time interval close to zero that may be written as

$$v(x,t)=\sum_{n=0}^{\infty}b_n(x)t^n$$

and (9)

$$\ln[n(x,t)]=\sum_{n=0}^{\infty}a_n(x)t^n\ .$$

Introducing Eq. (9) into the system (7) and (8) and equating the terms with the same power of t, the following recurrence relations are obtained:

$$(n+1)b_{n+1}+\sum_{j=1}^{n}b_j\frac{\delta b_{n-j}}{\delta x}=A_0\delta(n=0)-(kT/m)\frac{\delta a_n}{\delta x} \tag{10}$$

$$(n+1)a_{n+1}+\frac{\delta b_n}{\delta x}+\sum_{j=1}^{n}b_j\frac{\delta a_{n-j}}{\delta x}=0\ . \tag{11}$$

The initial conditions, for v and n, lead to $b_0=0$ and $a_0=\ln(n_0)-(x/\delta)^2$, from which it follows that $b_{2n}=0$ and $a_{2n+1}=0$.

From an inspection of the system of Eqs. (10) and (11), the following x dependence of a and b coefficients is derived:

$$a_{2n}(x)=a_{1,2n}+a_{2,2n}x+a_{3,2n}x^2\ , \tag{12}$$

$$b_{2n+1}(x)=b_{1,2n+1}+b_{2,2n+1}x\ , \tag{13}$$

where $a_{1,2n}$ and $b_{1,2n+1}$, independent of x, are defined by

$$\begin{aligned}
2na_{1,2n}&=(-1)^nB^2\beta_{2,2n-1}\\
&\quad-(-1)^n(A_0^2B^{n-2}/\delta^2)\sum_{j=0}^{n-1}\beta_{1,2j+1}\alpha_{2,2n-2-2j}\ ,\\
a_{2,2n}&=-(-1)^n(A_0B^{n-1}/\delta^2)\alpha_{2,2n}\ ,\\
a_{3,2n}&=-(-1)^n(B^n/\delta^2)\alpha_{3,2n}\ ,\\
b_{1,2n+1}&=(-1)^n(A_0B^n)\beta_{1,2n+1}\ ,\\
b_{2,2n+1}&=(-1)^nB^{n+1}\beta_{2,2n+1}\ .
\end{aligned} \tag{14}$$

Here $B=2kT/m\delta^2$ and α,β are numerical coefficients given by the system

$$\begin{aligned}
2n\alpha_{2,2n}&=2\sum_{j=0}^{n-1}\beta_{1,2j+1}\alpha_{3,2n-2-2j}\\
&\quad+\sum_{j=0}^{n-1}\beta_{2,2j+1}\alpha_{2,2n-2-2j}\ ,\\
n\alpha_{3,2n}&=\sum_{j=0}^{n-1}\beta_{2,2j+1}\alpha_{3,2n-2-2j}\ ,\\
(2n+1)\beta_{1,2n+1}&=\sum_{j=0}^{n-1}\beta_{1,2j+1}\beta_{2,2n-2j-1}+\alpha_{2,2n}\Big/2\ ,\\
(2n+1)\beta_{2,2n+1}&=\sum_{j=0}^{n-1}\beta_{2,2j+1}\beta_{2,2n-2j-1}+\alpha_{3,2n}\ ,
\end{aligned} \tag{15}$$

where $\alpha_{2,0}=0$, $\alpha_{3,0}=\beta_{1,1}=\beta_{2,1}=1$. The overall solution is greatly simplified by a remarkable relation among the coefficients in Eq. (15), that is,

$$\alpha_{3,2n}=\alpha_{2,2n+2} \tag{16}$$

from which results

$$\beta_{1,2n+1}=\tfrac{1}{2}\beta_{2,2n-1}\ , \tag{17}$$

$$\left[\frac{1}{2n}\right]\sum_{j=0}^{n-1}\beta_{1,2j+1}\alpha_{2,2n-2-2j}=\tfrac{1}{4}\alpha_{3,2(n-2)}\ . \tag{18}$$

After rearrangement of the indices, the solution may be expressed as

$$\ln(n/n_0)=\sum_{n=1}^{\infty}(-1)^n(\beta_{2,2n-1}/2n)\theta^n-[(\tfrac{1}{2}A_0t^2-x)/\delta]^2\sum_{n=0}^{\infty}(-1)^n\alpha_{3,2n}\theta^n\ , \tag{19}$$

$$v=A_0t+Bt(x-\tfrac{1}{2}A_0t^2)\sum_{n=0}^{\infty}(-1)^n\beta_{2,2n+1}\theta^n\ , \tag{20}$$

where it has been introduced that $\theta=Bt^2$.

The decrease in the numerical coefficients, with increasing n, does not assure the series convergence for $\theta\geq 1$. As a consequence, to describe the complete time evolution of v and $\ln(n)$, it will be necessary to find an analytic extension[15] of the series. Therefore, the series terms, in Eqs. (19) and (20), are written as unknown functions of the adimensional parameter θ,

$$\begin{aligned}
\sum_{n=1}^{\infty}(-1)^n(\beta_{2,2n-1}/2n)\theta^n&=\phi_1(\theta)\ ,\\
\sum_{n=0}^{\infty}(-1)^n\alpha_{3,2n}\theta^n&=\phi_2(\theta)\ ,\\
\sum_{n=0}^{\infty}(-1)^n\beta_{2,2n+1}\theta^n&=\phi_3(\theta)\ .
\end{aligned} \tag{21}$$

From the mass conservation and the other relations derived from the system (7) and (8), equating the terms with the same power of x, the following system is obtained:

$$\phi_1(\theta)=\tfrac{1}{2}\ln\phi_2(\theta)\ , \tag{22}$$

$$\phi_3=-\left[\frac{1}{2Bt\phi_2}\right]D\phi_2\ , \tag{23}$$

$$D^2\phi_2=\left[\frac{3}{2\phi_2}\right](D\phi_2)^2-2B\phi_2^2\ , \tag{24}$$

where D indicates the total time derivative. The initial conditions, for v and n, lead to $\phi_1(0)=\phi_3(0)=0$ and $\phi_2(0)=1$. By making use of Eq. (23), $D\phi_2\,|_{t=0}=0$ is obtained.

By introducing the variable $\theta=Bt^2$ in Eq. (24), it is easy to see that the shape of ϕ_2 is independent of the choice of the initial parameters. Thus $\phi_2(\theta)$ is a universal function describing, whatever the conditions of the MPI experiment, the spatial distribution of the ionized species. Figure 1 shows a bilogarithmic plot of θ_2 versus $(1+\theta)$, obtained by standard Runge-Kutta fourth-order numerical integration. The function ϕ_2 is well approximated by $1/(1+\theta)^{\alpha}$, where α is a weakly varying function of θ, approaching 1.25 at large θ values.

In conclusion, the complete solution will be expressed by

$$n/n_0=(\phi_2)^{1/2}\exp-\phi_2[(\tfrac{1}{2}A_0t^2-x)/\delta]^2\ , \tag{25}$$

$$v=A_0t+\tfrac{1}{2}(\tfrac{1}{2}A_0t^2-x)D\ln(\phi_2)\ . \tag{26}$$

The collective (pressure) effect is included in the ϕ_2 function. When $\theta\ll 1$, $\phi_2=1$, and thus the single-particle translation of a Gaussian profile is recovered. If $\theta\geq 1$, the universal ϕ_2 function describes the deviations from the single-particle behavior.

The fieldless ($A_0=0$) evolution, as obtained from Eqs. (25) and (26), is to be considered as an example of a self-similar motion.[16] In fact, a change of the initial parameters (kT,δ) and of the value of B, does not modify the shapes of n and v, but does modify the time scale of variation. This feature is a consequence of the particular choice of the initial density shape and it cannot be directly extended to an arbitrary profile.

From Eqs. (25) and (26) it follows that to avoid the collective pressure-induced motion for a collection at the point d with a time arrival $t=(2d/A_0)^{1/2}$, θ should be small as compared to 1 and the external electric field must satisfy the condition $E_0\gg 2kTd/e\delta^2$. Owing to the typical range of variation of δ (0.1–0.01 cm) in the MPI experiments, a strong electric field will be necessary to perform a fast and efficient charges collection. For instance, assuming $kT=1$ eV, $d=10$ cm, and $\delta=0.1$ cm, the above condition gives $E_0\gg 1800$ V/cm. In Sec. VI, as an example, the behavior of the peak of the current as a function of the electric field will be shown.

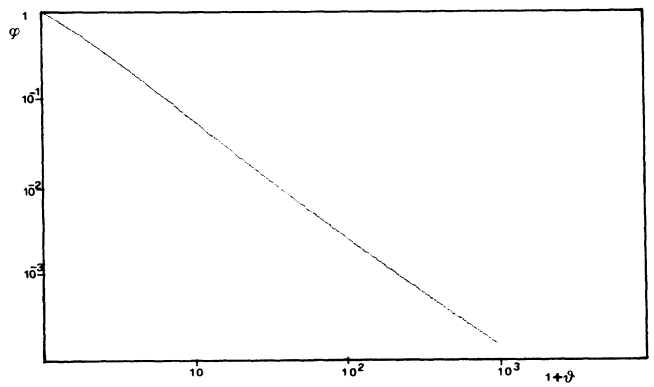

FIG. 1. Bilogarithmic plot of ϕ as a function of $(1+\theta)$.

III. EXTENSION OF THE SOLUTION

Since the previous solution depends only on the coordinate along the direction of the motion, a three-dimensional extension is straightforward. Moreover, the inclusion of momentum-exchange collisions with neutral particles, time-varying electric field, and temperature is very easy. In effect, the shapes of n and v are unchanged and the only modification results in the ϕ_2 time behavior and in the time-dependent term related to E_0.

The system to be solved, in the three-dimensional case, is

$$\frac{\delta\mathbf{v}}{\delta t}+(\mathbf{v}\cdot\nabla)\mathbf{v}=\mathbf{A}(t)-[kT(t)/m]\nabla\ln(n)-\beta\mathbf{v}\ , \tag{27}$$

$$\frac{\delta}{\delta t}\ln(n)+\nabla\cdot\mathbf{v}+(\mathbf{v}\cdot\nabla)\ln(n)=0\ . \tag{28}$$

The electric field will be assumed to be directed along the x axis: $\mathbf{A}(t)=(A(t),0,0)$.

For the solution of Eqs. (27) and (28), it may be noticed that the terms At and $(\frac{1}{2})At^2$, appearing in Eqs. (25) and (26), are to be replaced by the corresponding terms, obtained as a solution of the single-particle-like equation for the v_{0x} velocity,

$$Dv_{0x}=A(t)-\beta v_{0x}\ , \tag{29}$$

where D represents the total time derivative and β the collision frequency.

Furthermore, it is possible to take into account that the initial Gaussian shape could be nonisotropic by introducing Gaussian distributions with different widths δ_x, δ_y, and δ_z along the three axes. Thus the solution is written as

$$n/n_0=(\phi_x,\phi_y,\phi_z)^{1/2}\exp -\left\{\phi_x\left[\left[\int v_{0x}dt-x\right]\Big/\delta_x\right]^2+\phi_y(y/\delta_y)^2+\phi_z(z/\delta_z)^2\right\} \tag{30}$$

and

$$v_x=v_{0x}+(\tfrac{1}{2})\left[\int v_{0x}dt-x\right]D\ln\phi_x\ , \tag{31}$$

$$v_y=-(\tfrac{1}{2})yD\ln\phi_y\ , \tag{32}$$

$$v_z=-(\tfrac{1}{2})zD\ln\phi_z\ . \tag{33}$$

Replacing the solutions (30)–(33) into the system (27) and (28), and following the same procedure as in Sec. II, the differential equations, regulating the ϕ_j behavior, are

$$D^2\phi_j = \left[\frac{3}{2\phi_j}\right](D\phi_j)^2 - 2B_j(t)\phi_j^2 - \beta D\phi_j \ , \tag{34}$$

where j refers to the (x,y,z) direction of motion. Note that the time variation of the field affects the single-particle solution [Eq. (29)], whereas the time dependence of the temperature T appears only in Eq. (34), which modifies the time scale of the ϕ_j function, that is, it affects the collective behavior. On the contrary, the collision term influences the collective behavior [Eq. (34)] as well as the single-particle one [Eq. (29)].

As a further consequence, when $\beta \gg (B_j)^{1/2}$, the second derivative and the squared derivative may be neglected and Eq. (34) immediately gives the well-known result for a completely diffusional motion,[17] that is, $\phi_j = [1+(4kT/m\beta\delta^2)t]^{-1}$.

In many plasma physics problems, the nonlinear term $(\mathbf{v}\cdot\nabla)\mathbf{v}$ is often neglected. In such a case, the modification of the above solution concerns only the differential equation (34), where the numerical factor $\frac{3}{2}$ is to be replaced by 1.

In general, the previous solution, for the spatial dependence [Eqs. (12) and (13)], will not be valid in the presence of both a spatial dependence of E or T, and nonlinear terms in the continuity equation. Nevertheless, in the case of a linear spatial dependence of the electric field, it will be demonstrated that the previous solution is still valid (Sec. V).

IV. THE MAGNETOHYDRODYNAMIC PROBLEM

When the overall motion of the plasma is considered, the motion fluid equation for both ions and electrons include an electric field, given by the superposition of the external field and of the self-generated field, due to the different charge mobility. Hence, in general, the complete system to be solved also includes the Maxwell equations. In the standard MHD approach,[9] the above complete system is greatly simplified, under the assumption that the ion and electron densities are equal, except in the Poisson equation. The parameter measuring the range of validity of the above-mentioned hypothesis is the Debye length $\lambda \approx 7(T/n_e)^{1/2}$ cm whose value must be much smaller than the plasma characteristic length δ.[9]

It will be demonstrated that, in general, the MHD approach does not provide, owing to the strong density gradient in MPI-produced plasmas, a complete description of the time-space evolution of the macroscopic quantities. This is also true in the case where the neutrality condition ($\lambda \ll \delta$) is initially well verified. In any case, the MHD picture can give some information about the plasma motion at the initial times where the neutrality condition is still verified, and about the motion of the central zone, where the density gradient is smoother. Furthermore, the MHD approach will describe the limit behavior of those plasmas, with such an initial density that the neutrality condition would be verified anywhere and anytime.

If in the motion equation the nonlinear $(\mathbf{v}\cdot\nabla)\mathbf{v}$ term has been retained and all the terms and equations including the magnetic field are neglected, the MHD motion and Ohm equations are given, respectively, by

$$\frac{\delta\mathbf{v}}{\delta t} + (\mathbf{v}\cdot\nabla)\mathbf{v} = -[(kT_i + kT_e)/M]\nabla\ln(\rho) - \beta\mathbf{v} \ , \tag{35}$$

$$(Mm/e^2\rho)\left[\frac{\delta\mathbf{J}}{\delta t} + \beta\mathbf{J}\right] = \mathbf{E} + (1/e\rho)(M\nabla P_e - m\nabla P_i) \ , \tag{36}$$

where P_i and P_e represent, respectively, the ion and electron pressure terms, that is, $P_j = n_j kT_j$ $(j=i,e)$. The electric field $\mathbf{E}$ is given by $\mathbf{E} = \mathbf{E}_0 + \mathbf{E}_\rho$, where $\mathbf{E}_\rho$ is the self-generated electric field given by the Poisson equation

$$\nabla\cdot\mathbf{E}_\rho = 4\pi\sigma \ . \tag{37}$$

The further relevant equations are, for mass continuity,

$$\frac{\delta}{\delta t}\rho + \nabla\cdot(\rho\mathbf{v}) = 0 \ , \tag{38}$$

and for charge continuity,

$$\frac{\delta\sigma}{\delta t} + \nabla\cdot\mathbf{J} = 0 \ . \tag{39}$$

The new macroscopic quantities are related to the old variables by the system

$$\begin{aligned} &\rho = Mn_i + mn_e \ , \\ &\sigma = e(n_i - n_e) \ , \\ &\mathbf{v} = (M\mathbf{v}_i + m\mathbf{v}_e)/(M+m) \ , \\ &\mathbf{J} = e(n_i\mathbf{v}_i - n_e\mathbf{v}_e) \ . \end{aligned} \tag{40}$$

Equations (38) and (35) admit the general solution, expressed by the relations (30)–(33). Putting Eq. (37) into Eq. (40) and neglecting the pressure term $m\nabla P_i$ in Eq. (36), compared with $M\nabla P_e$, the system to solve is reduced to the following equations:

$$\frac{\delta\mathbf{J}}{\delta t} + \beta\mathbf{J} = (e^2/Mm)[\rho\mathbf{E} + (kT_e/e)\nabla\rho] \ , \tag{41}$$

$$(1/4\pi)\frac{\delta}{\delta t}\nabla\cdot\mathbf{E} + \nabla\cdot\mathbf{J} = 0 \ . \tag{42}$$

The one-dimensional case admits a straightforward solution. In fact, integrating Eq. (42) between $-\infty$, where both E_ρ and J are zero, and x, and making use of the Eq. (30) for ρ, the system (41) and (42) is reduced to the following time-dependent differential equation for E_ρ:

$$\frac{\delta^2 E_\rho}{\delta t^2} + \beta\frac{\delta}{\delta t}E_\rho + \Omega_{pe}^2\frac{\rho}{\rho_0}(x,t)E_\rho = -\Omega_{pe}^2\frac{\rho}{\rho_0}(x,t)E_0 + 4\pi eB_e\phi_2\rho x \ , \tag{43}$$

where $\Omega_{pe} = (4\pi e^2\rho_0/Mm)^{1/2}$ is the plasma frequency and $B_e = (2kT_e/m\delta^2)$.

The initial conditions for Eq. (43), are, of course,

$E_\rho(x,0)=0$ and $(\delta/\delta t)E\mid_{t=0}=0$.

Equation (43) represents an oscillating rotor-free electric field ("electrostatic"),[18] whose frequency is time-space varying, forced by the external electric field as well as by the internal field, owing to the different mobilities of charged particles. Note that a time dependence of the external electric field and temperature can be directly taken into account, as in Sec. III.

In the three-dimensional case, assuming a symmetric expansion of ρ, that is, $\delta_x=\delta_y=\delta_z$, the previous irrotational solution is still valid. Nevertheless, a typical MPI plasma is cylindrically symmetric and thus, also, a rotational solution will be expected, as experimentally observed, for instance, in Ref. 19, by the electromagnetic emission.

In any case, the one-dimensional picture is a suitable tool for analyzing the features of the MHD model and their range of validity. Since the time scale of variation of ρ is larger than the corresponding E_ρ scale by a factor $(M/m)^{1/2}$, neglecting the fast oscillating term and assuming $\beta=0$, Eq. (43) can be solved to obtain

$$E_\rho=[(2kT_e/e\delta^2)x-E_0][1-\cos(\Omega_{pe}f)t]\ , \tag{44}$$

where $f=\exp[-\frac{1}{2}(x/\delta)^2]$.

J is given by the time derivative of Eq. (38) and σ by the spatial derivative, that is,

$$J=\left[-\frac{1}{4\pi}\right][(2kT_e/e\delta^2)x-E_0]\Omega_{pe}f\sin(\Omega_{pe}f)t\ , \tag{45}$$

$$\sigma=\left[-\frac{1}{4\pi}\right]\{(2kT_e/e\delta^2)[1-\cos(\Omega_{pe}f)t]-(x/\delta^2)[(2kT_e/e\delta^2)x-E_0]\times\Omega_{pe}ft\sin(\Omega_{pe}f)t\}\ . \tag{46}$$

Figures 2(a) and 2(b) shows the spatial profile of $n_e=\rho/M+\sigma/e$, as a function of x/δ, at different time instants, chosen as multiples of the period $T=2\pi/\Omega_{pe}$. The ρ profile, also shown as a reference, is unchanged during the same time interval. The values of $kT_e=1$ eV, $N_0=10^{10}$ electrons/cm^3, and $\delta=0.1$ cm, introduced in Fig. 2(a), are common to most of the MPI experiments. Moreover, the neutrality condition $\lambda\ll\delta$ is initially well verified. Nevertheless, the very rapid growth of the charge separation suggests that the above-mentioned neutrality condition is not a suitable parameter. In fact, that condition is concerned only with the first term in Eq. (46), which represents the charge separation close to $x=0$. On the contrary, the most important contribution arises from the linear growing second term in Eq. (46). Thus, assuming as $\bar{t}$ the characteristic time of the ρ evolution ($\bar{t}\approx 3/B_1^{1/2}$) and $x=\delta$, the true neutrality condition becomes

$$N_0\gg(kT_e/4\pi\delta^2e^2)(M/m)\ , \tag{47}$$

that is, $\lambda\ll\delta(m/M)$. Assuming the previous values of the parameters and, for M, the proton mass, Eq. (47) gives $N_0\gg 3\times10^{12}$ ion/cm^3.

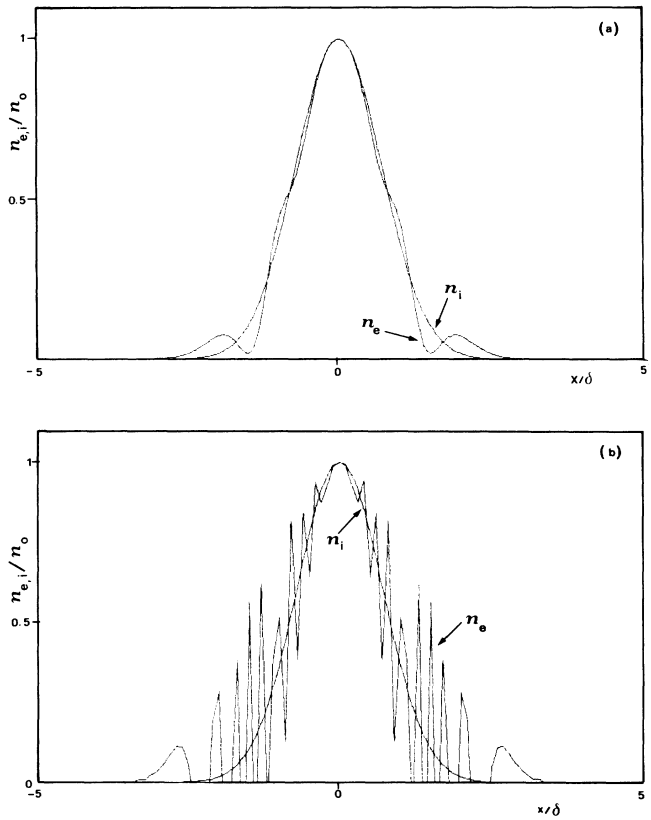

FIG. 2. Spatial profile of n_e and n_i vs x/δ from the MHD model at two different time instants. The electron energy is $kT_e=1$ eV and the initial charge density $N_0=10^{10}$ electrons/cm^3. (a) $t=4\pi/\Omega_{pe}$, (b) $t=20\pi/\Omega_{pe}$.

It follows that, for most of the MPI experiments, where the ion density is lower by several orders of magnitude, the MHD approach does not provide a suitable model for the macroscopic evolution. As a consequence, the two-fluid system seems the most appropriate approach to describe the physical reality. The previous solutions will be included as limit cases, depending on the experimental parameters (N,E,kT,δ).

V. SOLUTION OF THE TWO-FLUID SYSTEM

The system to solve is now a five-equation system, including two motion equations, coupled by the internal field, two continuity equations, and the Poisson equation which relates the internal self-generated field E_ρ with the ion and electron densities.[9] No additional hypothesis about the charge neutrality as in Sec. IV is assumed.

An exact solution is difficult to obtain, even by series development of Sec. II. In fact, owing to the coupling term E_ρ, the substitution $n\rightarrow\ln(n)$ is not allowed in the motion equations. Hence, the spatial dependence cannot be taken out in the simple way of Sec. II, and so a reduction of the recurrence relations becomes very difficult.

In any case, by restricting the treatment to the one-dimensional motion, a suitable solution may be obtained using a linearization of the Poisson equation. It will be demonstrated that, in such a case, only the differential

equations are modified, still supporting the general single-fluid solution [see Sec. III, Eqs. (30)–(33)].

Assuming the single-fluid shapes for both n_i and n_e, integrating between $-\infty$ and x, and by variable change $\epsilon_j=(\phi_j^{1/2}/\delta)(x_j-x)$, where the index j refers to both the species and $x_j(t)=\int v_{0j}dt$, the internal field is given by

$$E_\rho(x,t)=4\pi e n_0\delta\int_{\epsilon_i}^{\epsilon_e}\exp(-\epsilon^2)d\epsilon\ . \tag{48}$$

By series integration and retaining the first term, we obtain

$$E_\rho(x,t)=2\pi e n_0[(\phi_i^{1/2}-\phi_e^{1/2})x-\phi_i^{1/2}x_i+\phi_e^{1/2}x_e]\ . \tag{49}$$

Referring to the general single-fluid solution (Sec. III), it follows that the first term in Eq. (49), linearly depending on x, will affect the ϕ_i and ϕ_e time evolution, and the time-dependent term will modify the single-particle-like motion.

In fact, putting Eq. (49) into the motion and continuity equations and following the same procedure as in Sec. III, the following differential system is immediately obtained:

$$D^2\phi_i=(3/2\phi_i)(D\phi_i)^2-\Omega_{pi}^2\phi_i(\phi_i^{1/2}-\phi_e^{1/2})-2B_i\phi_i^2\ ,$$
$$D^2\phi_e=(3/2\phi_e)(D\phi_e)^2+\Omega_{pe}^2\phi_e(\phi_i^{1/2}-\phi_e^{1/2})-2B_e\phi_e^2\ , \tag{50}$$

and

$$D^2x_i=(e/M)E_0+\tfrac{1}{2}\Omega_{pi}^2\phi_e^{1/2}(x_e-x_i)\ ,$$
$$D^2x_e=-(e/m)E_0-\tfrac{1}{2}\Omega_{pe}^2\phi_i^{1/2}(x_e-x_i)\ , \tag{51}$$

where D represents the total time derivative. The initial conditions are the same as in Sec. II.

The above solution is a good approximation for the E_ρ field in a zone with length roughly δ. For $x>\delta$ the E_ρ field exhibits a strong decreasing to zero, at the charge boundary, faster than $\exp-\epsilon^2$ as obtained from the series integration in Eq. (49). Thus, this very narrow transition zone can be neglected without loss of generality and so the spatial profile will be divided in an inner zone, where the overlapping of both n_e and n_i makes the coupling term important, and an outer zone, where the motion will be single-fluid-like [in fact, for $\Omega_{pe}=\Omega_{pi}=0$, Eqs. (50) and (51) are reduced to the system (30) and (33)].

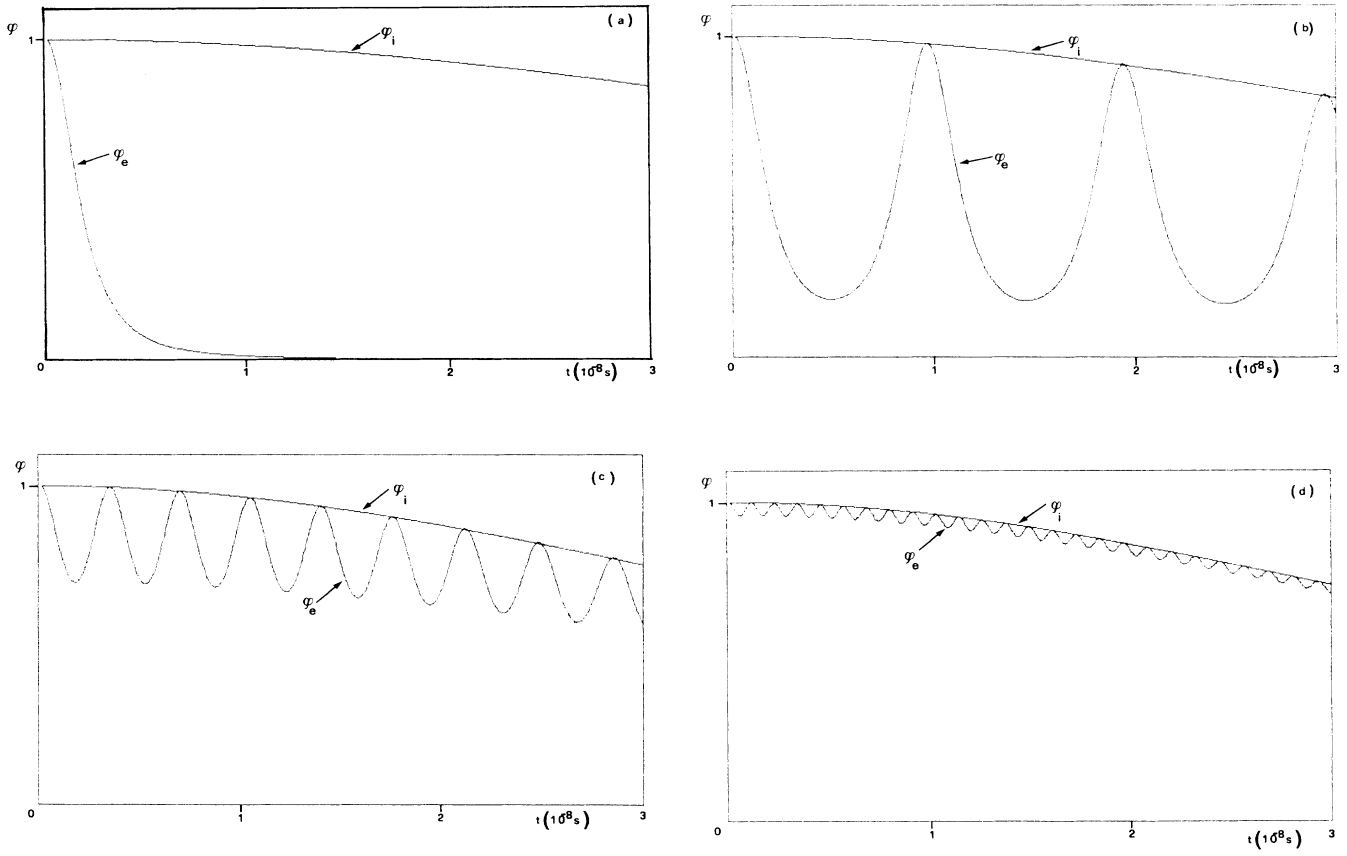

FIG. 3. ϕ_e and ϕ_i time evolution from the two-fluid model for $kT_e=1$ eV. (a) Uncoupled behavior. (b), (c), and (d) represent the effect of the coupling term at three different initial charge densities: (b) $N_0=10^8$ electrons/cm^3, (c) $N_0=10^9$ electrons/cm^3, and (d) $N_0=10^{10}$ electrons/cm^3.

The influence of the coupling term is shown in Figs. 3(a)–3(d), corresponding to different values of the initial plasma density.

The ϕ_e decreases until the coupling term equates the decreasing term $2B_e\phi_e^2$. The minimum of the ϕ_e function depends on the relevant parameters as

$$\phi_{e\min}=(\Omega_{pe}^4/8B_e^2\{[1+(4B_e\phi_i^{1/2}/\Omega_{pe}^2)] -[1+(8B_e\phi_i^{1/2}/\Omega_{pe}^2)]^{1/2}\}\ , \quad (52)$$

and the oscillation frequency is $\Omega\approx\Omega_{pe}\phi_i^{1/4}$. The coupling term also affects the ϕ_i behavior. Figure 4 shows the variation of the ϕ_i value, at a fixed time, as a function of the initial density and of the initial electron energy. The ϕ_i behavior indicates that there is a density region in which the plasma exhibits an unstable evolution. In fact, the faster decreasing of ϕ_i means that a fraction of electron energy is transferred to the ions.[20] As the density increases further up to the MHD region, the instability disappears, according to the results of Sec. IV.

Referring now to the previous discussion about the sharp boundary separating the two different behaviors, it will be noted that, when $\phi_{e\min}$ greatly differs from ϕ_i, only a fraction of electrons will be trapped in the ions zone. An estimate of this effect is given by

$$n_e/n_i=(\phi_{e\min}/\phi_i)^{(\Omega/4\pi)t}\ . \quad (53)$$

Figure 5 shows the behavior of Eq. (53). Comparison of Figs. 4 and 5 with Fig. 3(a) shows that trapping and instability begin to be important at the same value of the density, namely, $n>10^8$ ion/cm^3.

The coupling between electron and ion motion is also induced by the external field, as it shows the solution of the system (51), assuming $\phi_i=\phi_e=1$,

$$\begin{aligned} x_i&=M/(m+M)(E_0/4\pi en_0)\\ &\quad\times\{1-\cos[(M+m)/M]^{1/2}\Omega_{pe}t\}\\ &\quad-\tfrac{1}{2}[(M-m)/Mm]eE_0t^2\ ,\\ x_e&=-m/(m+M)(E_0/4\pi en_0)\\ &\quad\times\{1-\cos[(M+m)/M]^{1/2}\Omega_{pe}t\}\\ &\quad-\tfrac{1}{2}[(M-m)/Mm]eE_0t^2\ . \end{aligned} \quad (54)$$

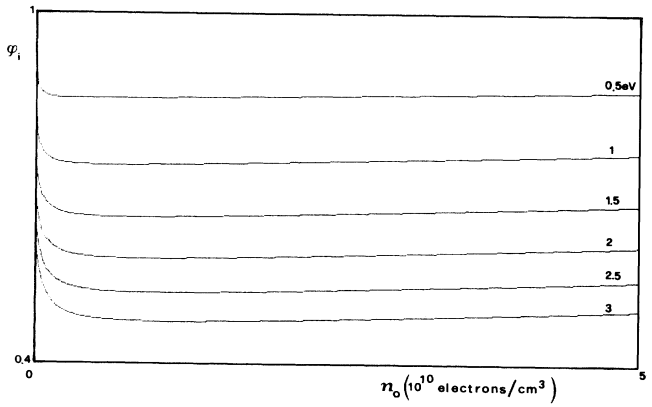

FIG. 4. ϕ_i value at $t=3\times10^{-8}$ sec as a function of the initial density, at different initial electron energies.

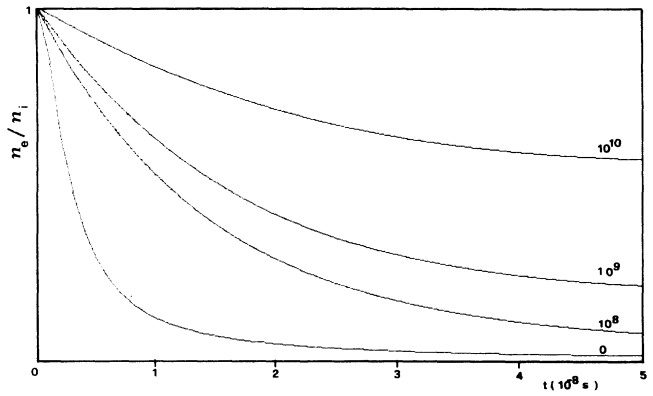

FIG. 5. Time evolution of the "trapping" factor (n_e/n_i) at different initial densities for $kT_e=1$ eV. The 0 line represents the ratio n_e/n_i deduced from the uncoupled evolution.

Compared with the MHD approach, the two-fluid model introduces a new effect, induced by the external field. If $B_e/\Omega_{pe}^2<1$, the ions are trailed at the initial time instants, when $\phi_i=\phi_e=1$, by the same acceleration as the electrons, and the relative distance (x_i-x_e) oscillates with an amplitude $E_0/4\pi n_0$.

This effect disappears in the further evolution, when both ϕ_i and ϕ_e decrease. The condition $B_e/\Omega_{pe}^2<1$ is equivalent to $\lambda/\delta<1$.

As n_0 decreases and the rate λ/δ decreases further, the two-fluid picture approximates the central behavior as pointed out in the MHD model. In fact, from Eq. (52), $\phi_{e\min}\to\phi_i$ implies $n_e/n_i\to1$ [Eq. (53)].

In the opposite limit $\lambda/\delta>1$, the influence of the coupling term becomes negligible and Eqs. (50) reduce to the uncoupled single-fluid equations and Eqs. (51) to the usual uniform accelerated motion for both ions and electrons.

VI. EXPERIMENTAL CONSEQUENCES OF THE COLLECTIVE MOTION

The aim of this section is to deduce, from the previous discussion, some general features about the macroscopic quantities. A more detailed comparison between theory and experiment is beyond the scope of this work.

As an example, Figs. 6(a) and 6(b) show the behavior of the maximum of the current at a fixed point, as a function of the external electric field, and for different initial electron energies, deduced from the one-dimensional single-fluid picture (Sec. II). In Fig. 7 the corresponding behavior of the collection time is shown. It is immediately inferred that, although the collection time agrees with the 0.5 slope (single particle) for reasonable values of the electric field, the maximum of the current strongly deviates. Moreover, the shape of the current pulse depends on the electric field value.

Particularly at a fixed electric field $E_0>6$ V/cm [Fig. 6(a)], the intensity of the peaks decreases as the initial electron energy increases, but, owing to the mass conser-

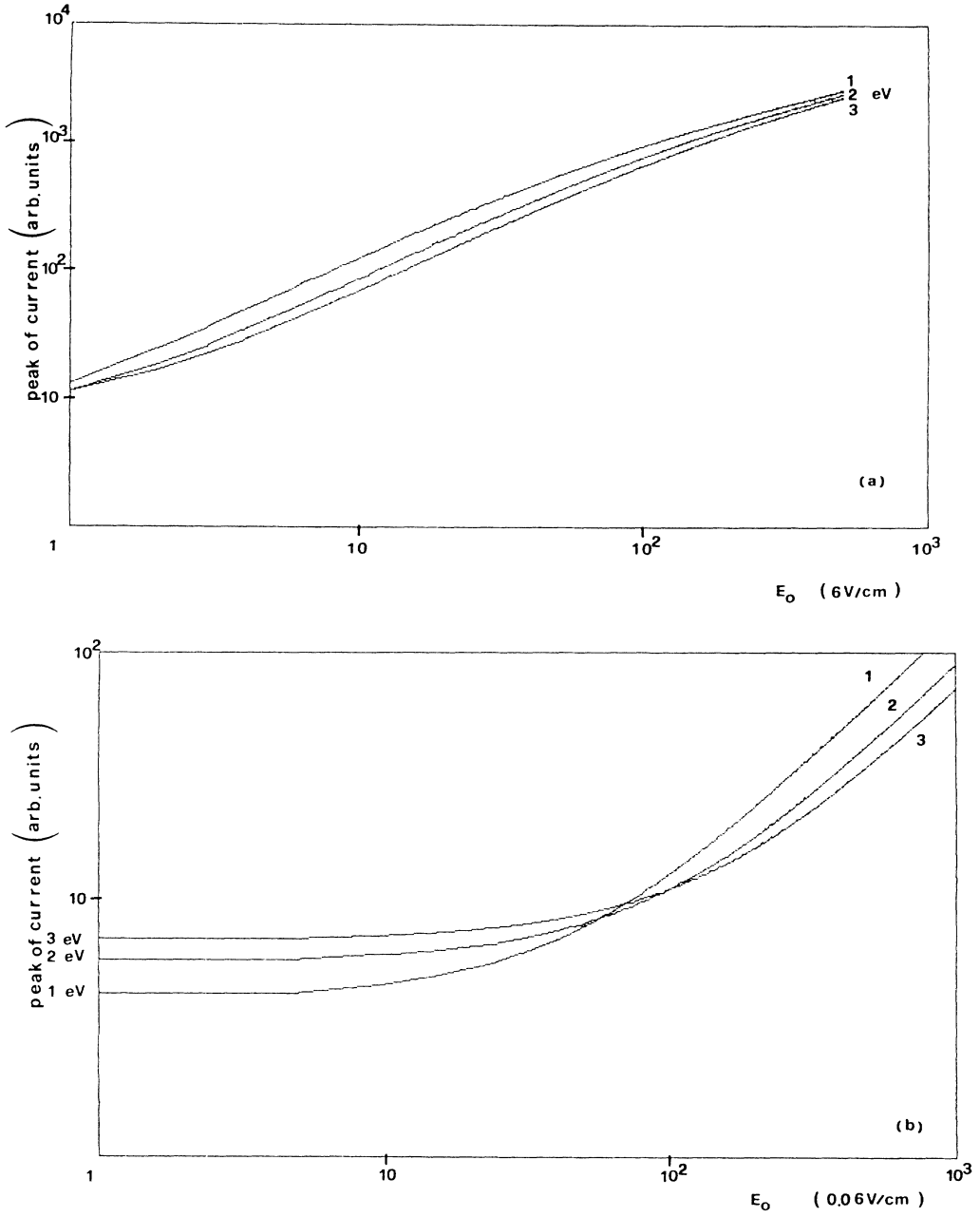

FIG. 6. Maximum of the current as a function of the external electric field from the single-fluid model, at a fixed collection point. (a) $6\ \text{V/cm} \leq E_0 \leq 6\times 10^3\ \text{V/cm}$, (b) $6\times 10^{-2}\ \text{V/cm} \leq E_0 \leq 60\ \text{V/cm}$.

vation, the current time integral retains a constant value. That implies an increasing broadening of the current time shape as the initial energy increases and also, from the point of view of the energy spectrum, a growth of the continuum background towards the low-energy region of the spectrum. For $E_0 < 6$ V/cm [Fig. 6(b)], the behavior is exactly opposite, and in the limit of $E_0 = 0$ the peaks depend on $(kT_e)^{1/2}$.

Following the outline of Sec. V, the two-fluid model could be suitable to treat the "electron trapping" effect recalled in the Introduction. As an example, Fig. 8 shows the effect on the charge collection induced by the "trapping" factor. The peaks are supposed to be produced initially at the same rate and propagate as a single-particle Gaussian profile, but present a strong broadening. Although Fig. 8 is derived from a very simplified approach, both the low-energy peaks lowering and the growth of the background, as observed in Refs. 4–8, increasing the charge density, appear clearly in the figure. Note that the trapping effect turns out to be important at a charge density of approximately 10^9 electrons/cm^3.

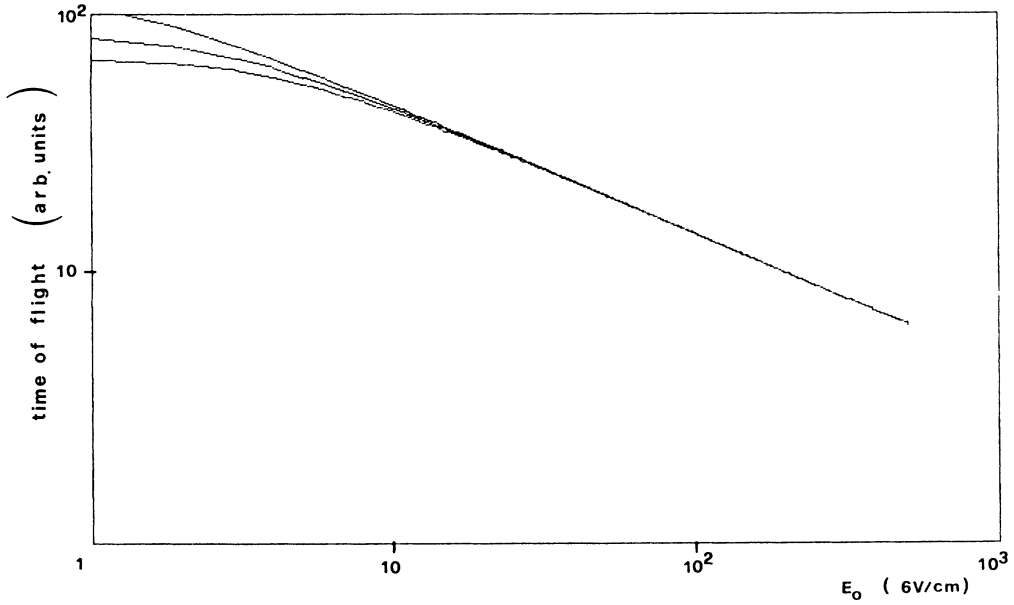

FIG. 7. Time arrival of the maximum of the current, at the collection point, as a function of the external electric field.

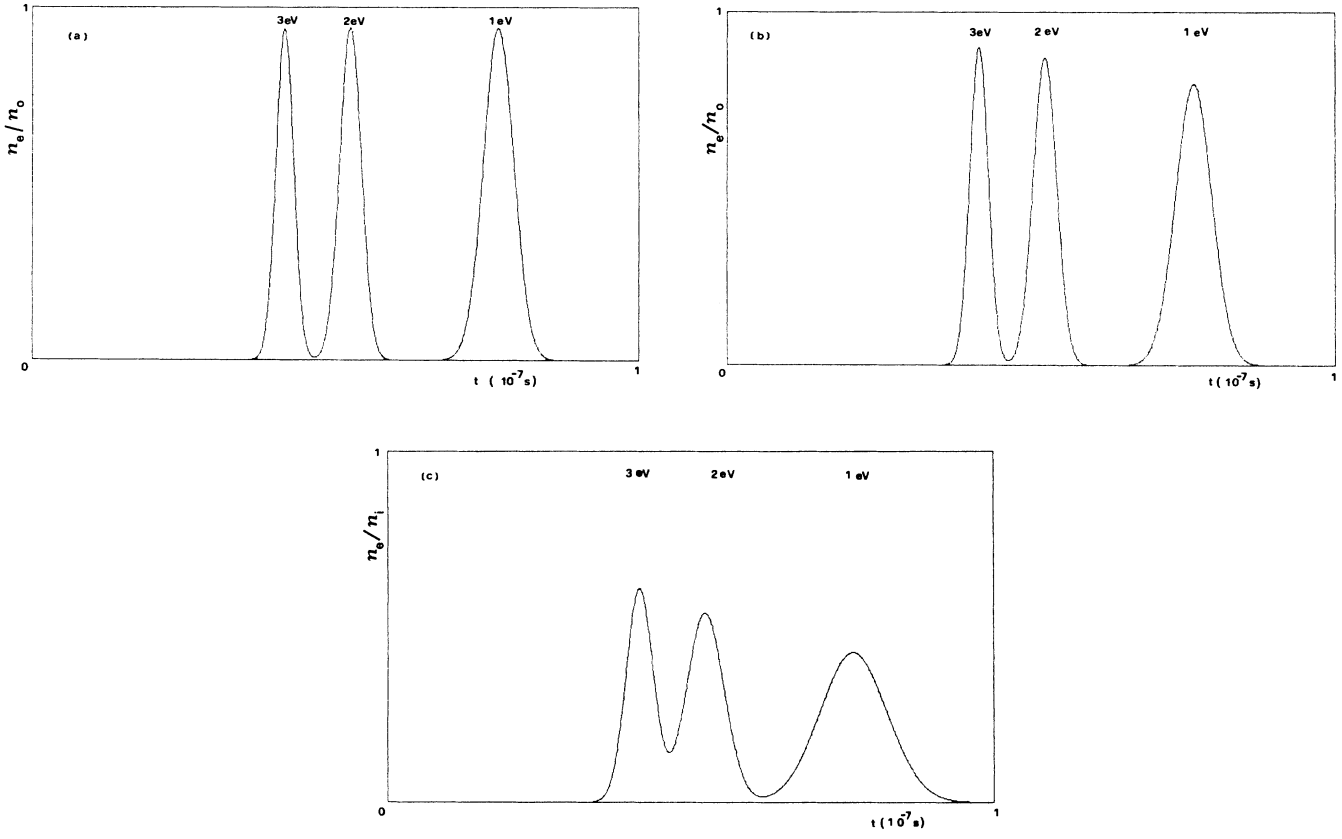

FIG. 8. Electron energy peaks at a fixed position for different initial energies 1 eV, 2 eV, 3 eV. (a) $N_0 = 10^8$ electrons/cm^3, (b) $N_0 = 10^9$ electrons/cm^3, (c) $N_0 = 10^{10}$ electrons/cm^3. The vertical axis is normalized to the initial density and the horizontal axis reports the collection time.

Moreover, in a complete description of the peak propagation, the pressure gradient effects must also be included. Referring to Fig. 6(b), the height of the peak current, at zero external electric field, depends on $E_e^{1/2}$, where E_e is the electron energy. Thus the signal width, owing to the mass conservation, increases with the decreasing of the electron energy. As a consequence, both the electron trapping and the pressure gradient effects cooperate with the suppression of the low-energy peaks and the growth of the continuum background towards the low-energy spectrum. Note that many hypotheses used in the previous discussion are consistent with the collecting field dispositions employed in the different experimental apparata. In fact, in Refs. 5 and 8 the electrons are driven along the detector direction by a magnetic field[21] that may be approximated as a one-dimensional free expansion. In other schemes, the electrons either freely expand through a retarded potential[6] or are weakly accelerated by an external electric field.[22,23] In any case, the applied fields are not so strong as to eliminate the pressure gradient effects (see Sec. II). As a consequence, the test generally used for the space-charge effect, i.e., an analysis of the signal variation versus the gas pressure,[6,22] could be rather ambiguous. In fact, whereas a sublinear slope surely indicates the presence of electron-ion coupling, the single-fluid picture also predicts a linear increasing in the presence of pressure gradient effect. Hence, it seems important that a more detailed analysis, taking into account the features of the different experiments, should be carried on in the future

To conclude the discussion of the current dependence on the laser power, the "volume" effects, due to the nonuniform distribution of the laser intensity near the focus, must also be taken into account. In fact, as the laser power increases, the external zones, not yet saturated, also contribute to the signal, giving an "anomalous" saturation slope.[24,25] This effect can be included in the theoretical analysis introducing a laser intensity dependence of the Gaussian δ width along the laser direction (see Sec. II). As the laser intensity increases, δ increases, smoothing the pressure gradient and lowering the expansion in the direction of the laser beam.

From the above discussion, it follows that the collection efficiency is greatly enhanced by three different effects: the increasing of the density in the focus, the increasing contribution of the not yet saturated external zones, and, finally, the δ change with the laser power which affects the characteristic time of expansion. Thus, the collective behavior introduces a further complication in the analysis of the experimental results concerning the studies of the atomic interaction.

The previous discussion concerns mainly the collective effects, deduced from the single-fluid approach. It is to be noted that many other effects may affect the charge collection. For instance, referring to the plasma evolution deduced in Sec. V, the increasing of the electron-ion interaction time, due to the "electron trapping" effect, will also enhance the influence of the electron-ion recombination.

VII. CONCLUSIONS

Following the previous discussion, the collective effects cannot be neglected in most MPI experiments, and thus strongly complicate the check of the theoretical predictions about the laser interaction at the atomic scale. The lowering of the charge density, below the density threshold of the collective behavior, in many cases is limited by the signal-to-noise ratio of the experimental set-up. In other cases, the investigated effects (for instance, chemical reactions) disappear at too low a density level.

Hence, it seems important when the collective limit is unavoidable that the plasma parameters are measured in an independent way, adding a plasma diagnostic to the standard apparatus, In such a way, a suitable collective model could be performed to analyze separately the effect of the laser interaction.

On the contrary, from the plasma physics point of view, the MPI-produced plasma constitutes a very suitable sample to study nonlinear phenomena. As pointed out in Sec. V, in the density region among 10^8–10^{11} ion/cm^3 the plasma exhibits macroscopic instabilities both internal, due to the different electron-ion mobilities, and external, induced by the external electric field. Moreover, the electromagnetic and electrostatic behavior could be studied, for instance, as a diagnostic method in a density region, where the standard methods fail.

Finally, it will be noted that much work must still be done to extend the previous solutions to include motion in a magnetic field or in a spatially nonuniform electric field, and also to take into account the collision terms changing the number density in the continuity equation. For the above-mentioned extension, the previous solutions can be considered as a sort of "homogeneous" solution, and the increasing importance of the added terms may be deduced from it, for instance, by perturbative methods.

ACKNOWLEDGMENTS

The author is greatly indebted to Professor E. Arimondo and Professor N. Rahman for helpful discussions and suggestions.

[1]For a review see Proceedings of the Third International Symposium on Resonance Ionization Spectroscopy and Application, Swansea, United Kingdom, 1986 (Hilger, London, in press). Also see Ref. 2.

[2]Proceedings of the Colloquium on Optogalvanic Spectroscopy, Aussois, France, 1983 [J. Phys. (Paris) Colloq. **C7**, 44 (1983)].

[3]M. Crance, J. Phys. B **19**, L267 (1986).

[4]B. Carre, F. Roussel, G. Spiess, J. M. Bizau, P. Gerard, and F. Wuilleumier, Z. Phys. D **1**, 79 (1986).

[5]F. Yergeau, G. Petite, and P. Agostini, J. Phys. B **19**, L663

(1986).
[6]L. A. Lompre, A. L'Huillier, G. Mainfray, and C. Manus, J. Opt. Soc. Am. B **2**, 1906 (1985).
[7]P. H. Bucksbaum, M. Bashkansky, R. R. Freeman, and T. J. McIlrath, Phys. Rev. Lett. **56**, 24 (1986).
[8]P. Kruit, J. Kimman, H. G. Muller, and M. J. van der Wiel, Phys. Rev. A **28**, 248 (1983).
[9]L. Spitzer, *Physics of Fully Ionized Gases* (Interscience, New York, 1956); L. D. Landau and E. M. Lifshitz, *Kinetics Physics* (Mir, Moscow, 1979).
[10]G. Leuchs, J. Reif, and H. Walther, J. Appl. Phys. B **28**, 87 (1982).
[11]H. J. Humpert, H. Schwier, R. Hippler, and H. O. Lutz, Phys. Rev. A **32**, 3787 (1985).
[12]A. Dodhy, R. N. Compton, and J. A. D. Stockdale, Phys. Rev. Lett. **54**, 5 (1985).
[13]F. Fabre, P. Agostini, G. Petite, and M. Clement, J. Phys. B **14**, L677 (1981).
[14]G. Petite, F. Fabre, P. Agostini, M. Crance, and M. Aymar, Phys. Rev. A **29**, 2677 (1984).
[15]A. Erdelyi, *Asymptotic Expansions* (Dover, New York, 1956).
[16]Ya. B. Zel'dovich and Yu. P. Raizer, *Physics of Shock Waves and High-Temperature Hydrodynamic Phenomena* (Academic, New York, 1966).
[17]L. D. Landau and E. M. Lifshitz, *Mecanique des Fluides* (Mir, Moscow, 1971).
[18]A. I. Akhiezer, *Collective Oscillations in a Plasma* (Pergamon, New York, 1967).
[19]A. M. Davtyan, R. Kh. Drampyan, and M. E. Movsesyan, Kvant. Elektron. (Moscow) **11**, 1003 (1984) [Sov. J. Quantum Electron. **14**, 5 (1984)].
[20]R. C. Davidson, *Theory of Non-Neutral Plasmas* (Benjamin, Reading, Mass., 1974).
[21]P. Kruit and F. H. Read, J. Phys. E **16**, 313 (1983).
[22]P. Agostini, M. Clement, F. Fabre, and G. Petite, J. Phys. B **14**, L491 (1981).
[23]F. Fabre, G. Petite, P. Agostini, and M. Clement, J. Phys. B **15**, 1353 (1982).
[24]J. M. Salter, D. D. Burgess, and N. A. Ebrahim, J. Phys. B **12**, L759 (1979).
[25]F. Giammanco and S. Gozzini, Nuovo Cimento B **66**, 1 (1981).